

# Nuclear matter properties and relativistic mean-field theory

 K.C. Chung<sup>1,a</sup>, C.S. Wang<sup>1,2</sup>, A.J. Santiago<sup>1</sup>, and J.W. Zhang<sup>2</sup>
<sup>1</sup> Instituto de Física, Universidade do Estado do Rio de Janeiro, Rio de Janeiro-RJ 20559-900, Brazil

<sup>2</sup> Department of Technical Physics, Peking University, Beijing 100871, China

Received: 5 May 2000 / Revised version: 23 November 2000

Communicated by A. Molinari

**Abstract.** Nuclear matter properties are calculated in the relativistic mean-field theory by using a number of different parameter sets. The result shows that the volume energy  $a_1$  and the symmetry energy  $J$  are around the acceptable values 16 MeV and 30 MeV, respectively; the incompressibility  $K_0$  is unacceptably high in the linear model, but assumes reasonable value if nonlinear terms are included; the density symmetry  $L$  is around 100 MeV for most parameter sets, and the symmetry incompressibility  $K_s$  has positive sign which is opposite to expectations based on the nonrelativistic model. In almost all parameter sets there exists a critical point  $(\rho_c, \delta_c)$ , where the minimum and the maximum of the equation of state are coincident and the incompressibility equals zero, falling into ranges  $0.014 \text{ fm}^{-3} < \rho_c < 0.039 \text{ fm}^{-3}$  and  $0.74 < \delta_c \leq 0.95$ ; for a few parameter sets there is no critical point and the pure neutron matter is predicted to be bound. The maximum mass  $M_{\text{NS}}$  of neutron stars is predicted in the range  $2.45M_{\odot} \leq M_{\text{NS}} \leq 3.26M_{\odot}$ , the corresponding neutron star radius  $R_{\text{NS}}$  is in the range  $12.2 \text{ km} \leq R_{\text{NS}} \leq 15.1 \text{ km}$ .

**PACS.** 21.65.+f Nuclear matter – 24.10.Jv Relativistic models – 26.60.+c Nuclear matter aspects of neutron stars

## 1 Introduction

Ground-state nuclear matter properties are specified by the nuclear matter equation of state  $e(\rho_N, \delta)$  which is simply the energy per nucleon of nuclear matter given as a function of nucleon density  $\rho_N$  and relative neutron excess  $\delta = (\rho_n - \rho_p)/\rho_N$ . This equation of state is a fundamental quantity in theories of neutron stars and supernova explosions, as well as in theories of nucleus-nucleus collisions at energies where nuclear compressibility comes into play [1]. The main measured quantities which can provide information about equation of state are the binding energies and other data from finite nuclei. As the finite nuclei are in states near the nuclear matter standard state  $(\rho_N = \rho_0, \delta = 0)$ , which is defined as the equilibrium state of symmetric nuclear matter with minimum energy per nucleon and called also the normal state, our actual knowledge of nuclear matter is mainly about nuclear matter at state close to the point  $(\rho_0, 0)$ . In this case, the equation of state can be written approximately as [2,3]

$$e(\rho_N, \delta) = -a_1 + \frac{1}{18}(K_0 + K_s\delta^2)\left(\frac{\rho_N - \rho_0}{\rho_0}\right)^2 + \left[J + \frac{L}{3}\left(\frac{\rho_N - \rho_0}{\rho_0}\right)\right]\delta^2, \quad (1)$$

which is specified by the standard density  $\rho_0$ , volume energy  $a_1$ , symmetry energy  $J$ , incompressibility  $K_0$ , density symmetry  $L$  and symmetry incompressibility  $K_s$ . The most interesting quantity for supernova explosion calculation is the nuclear incompressibility  $K_0$  which dictates the balance between gravity and internal pressure of the stellar system, while the most interesting quantities for heavy-ion collision studies are the nuclear incompressibility  $K_0$  and the symmetry incompressibility  $K_s$  which influence the side-flow effects and the isotopic distributions of the collisions, respectively.

There is no direct experimental measurement on these quantities. They can be determined only from data fit based on some specific nuclear model. Therefore, our actual knowledge about these quantities is essentially model dependent. Nowadays the quantities which are known with reasonable precision are  $a_1$ ,  $J$  and  $K_0$ , being the last two still under active investigation. One of the most sophisticated data fit is given by the nonrelativistic Thomas-Fermi statistical model of nuclei with Myers-Swiatecki phenomenological nucleon-nucleon interaction [4]. It is a fit to 1654 ground-state masses of nuclei with  $N, Z \geq 8$ , together with a constraint that ensures agreement with measured values of the nuclear surface diffuseness, giving the root-mean-square mass deviation equal to 0.655 MeV. The data fits based on Skyrme nucleon-nucleon interactions give comparable results [3], whereas a model independent but approximate data fit also gives  $a_1$ ,  $K_0$ ,  $J$  and

---

<sup>a</sup> e-mail: chung@uerj.br

$L$  very close to that obtained by the before-mentioned data fit [5, 6].

As the  $\sigma$ - $\omega$ - $\rho$  model of the relativistic mean-field theory is used widely to investigate various nuclear phenomena with success [7–10], it is interesting to calculate these nuclear matter quantities within this model by using the available parameter sets, to compare with those obtained by the nonrelativistic model. In addition, as these parameters are determined by nuclear ground-state properties, it is also interesting to see what the  $\sigma$ - $\omega$ - $\rho$  model can predict for the nuclear system under extreme conditions of density and asymmetry. In this case, the most interesting quantities are the location  $e_m = e(\rho_m, \delta)$  of the minimum of the equation of state for given asymmetry  $\delta$ , and the generalized incompressibility  $K_m = K(\rho_m, \delta)$  of the nuclear matter at this state [11]. Another interesting quantity is the maximum mass of neutron stars  $M_{\text{NS}}$  calculated by the equation of state for neutron matter with  $\delta = 1$ . Actually, to predict these properties of nuclear matter under extreme conditions is just one of the main goals in developing a relativistic mean-field theory [9].

The purpose of this paper is to make the above-mentioned calculation in comparing with results obtained by the nonrelativistic model. Section 2 presents the formalism and formulas used in this calculation. Section 3 addresses a numerical analysis on linear  $\sigma$ - $\omega$ - $\rho$  model of the relativistic mean-field theory. The standard nuclear matter properties calculated from a number of parameter sets are given in section 4, and the prediction for cold nuclear matter under extreme conditions is made in section 5. Section 6 gives the summary. Appendix A displays functions  $F_m(x)$  and  $f_m(x)$  which are useful in the analytical expressions as well as in the numerical calculations. The Bjorken-Drell convention for four-vector [12] and the natural units with  $\hbar = c = 1$  are used.

## 2 Formalism

The  $\sigma$ - $\omega$ - $\rho$  model of the relativistic mean-field theory is specified by the following Lagrangian density [9]:

$$\begin{aligned} \mathcal{L} = & \bar{\psi} [\gamma_\mu (i\partial^\mu - g_\omega \omega^\mu - g_\rho \boldsymbol{\tau} \cdot \mathbf{b}^\mu) - (M - g_\sigma \phi)] \psi \\ & + \frac{1}{2} (\partial_\mu \phi \partial^\mu \phi - m_\sigma^2 \phi^2) - \frac{1}{3} M b (g_\sigma \phi)^3 - \frac{1}{4} c (g_\sigma \phi)^4 \\ & - \frac{1}{4} F_{\mu\nu} F^{\mu\nu} + \frac{1}{2} m_\omega^2 \omega_\mu \omega^\mu + \frac{1}{4} c_3 (\omega_\mu \omega^\mu)^2 \\ & - \frac{1}{4} \mathbf{B}_{\mu\nu} \cdot \mathbf{B}^{\mu\nu} + \frac{1}{2} m_\rho^2 \mathbf{b}_\mu \cdot \mathbf{b}^\mu, \end{aligned} \quad (2)$$

where  $F^{\mu\nu} = \partial^\mu \omega^\nu - \partial^\nu \omega^\mu$ ,  $\mathbf{B}^{\mu\nu} = \partial^\mu \mathbf{b}^\nu - \partial^\nu \mathbf{b}^\mu$ ,  $\psi$ ,  $\phi$ ,  $\omega$  and  $\mathbf{b}^\mu$  are the nucleon,  $\sigma$ -,  $\omega$ - and  $\rho$ -meson fields with masses  $M$ ,  $m_\sigma$ ,  $m_\omega$  and  $m_\rho$ , respectively, while  $g_\sigma$ ,  $g_\omega$  and  $g_\rho$  are the respective coupling constants;  $b$ ,  $c$  and  $c_3$  are the nonlinear term coefficients, and  $\boldsymbol{\tau}$  are isospin matrices. The nuclear matter equation of state derived from this Lagrangian density can be expressed in terms of the nuclear

energy density  $\mathcal{E}$  as  $e = \mathcal{E}/\rho_{\text{N}} - M$ , and

$$\mathcal{E} = \mathcal{E}_k + \mathcal{E}_\sigma + \mathcal{E}_\omega + \mathcal{E}_\rho, \quad (3)$$

$$\mathcal{E}_k = \frac{M^4 \xi^4}{\pi^2} \sum_{i=p,n} F_1(k_i/\xi M), \quad (4)$$

$$\mathcal{E}_\sigma = M^4 \left[ \frac{1}{2C_\sigma^2} (1 - \xi)^2 + \frac{1}{3} b (1 - \xi)^3 + \frac{1}{4} c (1 - \xi)^4 \right], \quad (5)$$

$$\begin{aligned} \mathcal{E}_\omega = & \frac{C_\omega^2 \rho_{\text{N}}^2}{2M^2} \frac{1}{(1 + c_3 \omega_0^2/m_\omega^2)} \\ & + c_3 \frac{3}{4} \frac{C_\omega^4 \rho_{\text{N}}^4}{M^4 m_\omega^4} \frac{1}{(1 + c_3 \omega_0^2/m_\omega^2)^4}, \end{aligned} \quad (6)$$

$$\mathcal{E}_\rho = \frac{C_\rho^2 \rho_{\text{N}}^2}{2M^2} \delta^2, \quad (7)$$

where  $k_p$  and  $k_n$  are the proton and neutron Fermi momenta, respectively,

$$\xi = \frac{M^*}{M} = 1 - \frac{g_\sigma}{M} \phi, \quad (8)$$

$$C_i = g_i \frac{M}{m_i}, \quad i = \sigma, \omega, \rho, \quad (9)$$

and the function  $F_m(x)$  is defined as (see appendix A for details):

$$F_m(x) = \int_0^x dx x^{2m} \sqrt{1 + x^2}. \quad (10)$$

The reduced effective nucleon mass  $\xi$  and thus the field  $\phi$  is determined by

$$\begin{aligned} (1 - \xi) + b C_\sigma^2 (1 - \xi)^2 + c C_\sigma^2 (1 - \xi)^3 = \\ \frac{C_\sigma^2}{\pi^2} \xi^3 \sum_{i=p,n} f_1(k_i/\xi M), \end{aligned} \quad (11)$$

and the field  $\omega_0$  by

$$\omega_0 = \frac{C_\omega \rho_{\text{N}}}{M m_\omega} \frac{1}{1 + c_3 \omega_0^2/m_\omega^2}. \quad (12)$$

Knowing the equation of state, the following formulas for pressure  $p$  and generalized incompressibility  $K$  [11] can be obtained:

$$\begin{aligned} p = -\mathcal{E} + \rho_{\text{N}} \frac{\partial \mathcal{E}}{\partial \rho_{\text{N}}} = \\ \frac{1}{3} \mathcal{E}_k - \frac{1}{3} M \xi \rho_{\text{N}} - \mathcal{E}_\sigma + \mathcal{E}_\omega - \frac{1}{2} c_3 \omega_0^4 + \mathcal{E}_\rho, \end{aligned} \quad (13)$$

$$\begin{aligned} K \equiv 9 \frac{\partial p}{\partial \rho_{\text{N}}} = \frac{1}{\rho_{\text{N}}} \left\{ \frac{M^4 \xi^4}{\pi^2} \sum_{i=p,n} \left( \frac{k_i}{\xi M} \right)^3 f_1'(k_i/\xi M) \right. \\ \left. + 9 \frac{C_\rho^2 \rho_{\text{N}}^2}{M^2} \delta^2 + 9 \frac{C_\omega^2 \rho_{\text{N}}^2}{M^2} \frac{1}{1 + 3c_3 \omega_0^2/m_\omega^2} \right. \\ \left. + 3 \frac{M^4 \xi^4}{\pi^2} \sum_{i=p,n} \frac{k_i}{\xi M} f_1'(k_i/\xi M) \frac{\rho_{\text{N}}}{\xi} \frac{\partial \xi}{\partial \rho_{\text{N}}} \right\}, \end{aligned} \quad (14)$$

$$\frac{\rho_N}{\xi} \frac{\partial \xi}{\partial \rho_N} = \frac{1}{3} \frac{Q}{\xi [1 + 2bC_\sigma^2(1-\xi) + 3cC_\sigma^2(1-\xi)^2] + Q + 3C_\sigma^2\rho_s/M^3}, \quad (15)$$

$$\rho_s = \frac{M^3 \xi^3}{\pi^2} \sum_{i=p,n} f_1(k_i/\xi M), \quad (16)$$

$$Q = -\frac{C_\sigma^2}{\pi^2} \xi^3 \sum_{i=p,n} \frac{k_i}{\xi M} f'_1(k_i/\xi M). \quad (17)$$

In the previous equation where  $f'_m(x) = df_m(x)/dx$ , and the function  $f_m(x)$  is defined as (see appendix A for details)

$$f_m(x) = \int_0^x dx \frac{x^{2m}}{\sqrt{1+x^2}}. \quad (18)$$

At the standard state  $(\rho_0, 0)$ , the pressure should be zero,

$$p(\rho_0, 0) = 0, \quad (19)$$

and

$$K_0 = K(\rho_0, 0) = 9 \left( \rho_N^2 \frac{\partial^2 e}{\partial \rho_N^2} \right)_0. \quad (20)$$

In addition, the following formulas can be derived:

$$J \equiv \frac{1}{2} \frac{\partial^2 e}{\partial \delta^2} \Big|_0 = \frac{1}{6} \frac{k_F^2}{\sqrt{k_F^2 + M^2 \xi_0^2}} + \frac{C_\rho^2 k_F^3}{3\pi^2 M^2}, \quad (21)$$

$$L \equiv \frac{3}{2} \left( \rho_N \frac{\partial^3 e}{\partial \rho_N \partial \delta^2} \right)_0 = J + 2J_\rho - \left\{ 3 + \frac{M^3}{C_\sigma^2 \rho_s} \xi [1 + 2bC_\sigma^2(1-\xi) + 3cC_\sigma^2(1-\xi)^2] \right\} J_\sigma, \quad (22)$$

$$J_\rho = \frac{C_\rho^2 \rho_0}{2M^2}, \quad (23)$$

$$J_\sigma = -\frac{3}{2} M \left( \frac{M \xi_0}{k_F} \right)^3 f_1(k_F/\xi_0 M) \frac{\partial^2 \xi}{\partial \delta^2} \Big|_0, \quad (24)$$

$$\begin{aligned} \frac{\partial^2 \xi}{\partial \delta^2} \Big|_0 &= \frac{2}{9} \frac{C_\sigma^2 \xi_0^3}{\pi^2} \\ &\times \left[ 2 \frac{k}{\xi M} f'_1(k/\xi M) - \left( \frac{k}{\xi M} \right)^2 f''_1(k/\xi M) \right]_0 \\ &\times \left\{ \frac{2C_\sigma^2 \xi_0^2}{\pi^2} \left[ 3f_1(k/\xi M) - \frac{k}{\xi M} f'_1(k/\xi M) \right] \right. \\ &\left. + [1 + 2bC_\sigma^2(1-\xi) + 3cC_\sigma^2(1-\xi)^2] \right\}_0^{-1}, \quad (25) \end{aligned}$$

$$K_s \equiv \frac{9}{2} \left( \rho_N^2 \frac{\partial^4 e}{\partial \rho_N^2 \partial \delta^2} \right)_0 = -6L + \frac{1}{2} \frac{\partial^2 K}{\partial \delta^2} \Big|_0. \quad (26)$$

The subscript 0 in the above formulas stands for the standard state  $(\rho_0, 0)$ , and  $k_F$  is the nucleon Fermi momentum of standard nuclear matter which is related to standard density  $\rho_0$  and nuclear radius constant  $r_0$  as

$$\rho_0 = \frac{1}{4\pi r_0^3/3} = \frac{2k_F^3}{3\pi^2}. \quad (27)$$

Formula (21) is well-known in the literature [7]. It is worthwhile to note that, for the linear model with  $b = c = c_3 = 0$ , the  $\rho$ -meson in the standard state is nonrelevant to eqs. (3), (11) and (19). Thus the parameters  $C_\sigma$  and  $C_\omega$  are the same both for model with or without  $\rho$ -meson, since they are determined by standard density  $\rho_0$  and volume energy  $a_1$ . This point will be discussed more specifically in the next section.

### 3 Determination of $C_\sigma$ , $C_\omega$ and $C_\rho$ in the linear model

For the linear model,  $b = c = c_3 = 0$ , the nuclear energy density (3) in the standard state  $(\rho_0, 0)$  is simplified as

$$\mathcal{E}_0 = 2 \frac{M^4 \xi_0^4}{\pi^2} F_1(k_F/\xi_0 M) + \frac{M^4}{2C_\sigma^2} (1 - \xi_0)^2 + \frac{C_\omega^2 \rho_0^2}{2M^2}, \quad (28)$$

and eq. (11) determining the reduced effective nucleon mass  $\xi$  becomes

$$1 - \xi_0 = 2 \frac{C_\sigma^2 \xi_0^3}{\pi^2} f_1(k_F/\xi_0 M). \quad (29)$$

In addition, the equilibrium condition (19) and the expression of incompressibility (20) are reduced, respectively, to

$$\frac{2}{3} \frac{M^4 \xi_0^4}{\pi^2} f_2(k_F/\xi_0 M) - \frac{M^4}{2C_\sigma^2} (1 - \xi_0)^2 + \frac{C_\omega^2 \rho_0^2}{2M^2} = 0, \quad (30)$$

$$K_0 = 6 \frac{C_\omega^2 k_F^3}{\pi^2 M^2} + 3M \xi_0 f'_1(k_F/\xi_0 M) \times \left[ 1 + \frac{M^2 \xi_0^2}{k_F^2} \left( \frac{Q_0}{3 - 2\xi_0 + Q_0} \right) \right], \quad (31)$$

$$Q_0 = -2 \frac{C_\sigma^2 \xi_0^3}{\pi^2} \frac{k_F}{\xi_0 M} f'_1(k_F/\xi_0 M). \quad (32)$$

It can be seen from eqs. (28)–(32) that the relevant quantities are  $k_F$ ,  $C_\sigma^2$ ,  $C_\omega^2$  and  $M$ . Note that  $\xi_0$  is determined by eq. (29) and  $\rho_0$  is related to  $k_F$  by eq. (27). Therefore, as the measured nucleon mass can be taken for  $M$ , the composite parameters  $C_\sigma^2$  and  $C_\omega^2$  can be determined completely by the value  $e_0 = e(\rho_0, 0)$ , by using eqs. (28)–(30) together with  $\mathcal{E}_0 = (e_0 + M)\rho_0$ . The procedure is as follows.

At the stable equilibrium point  $(\rho_0, 0)$ , an equation involving  $e_0$ ,  $k_F$ ,  $\xi_0$  and  $C_\sigma$  can be obtained if eqs. (28) and (30) are combined to cancel  $C_\omega$ . On the other hand,

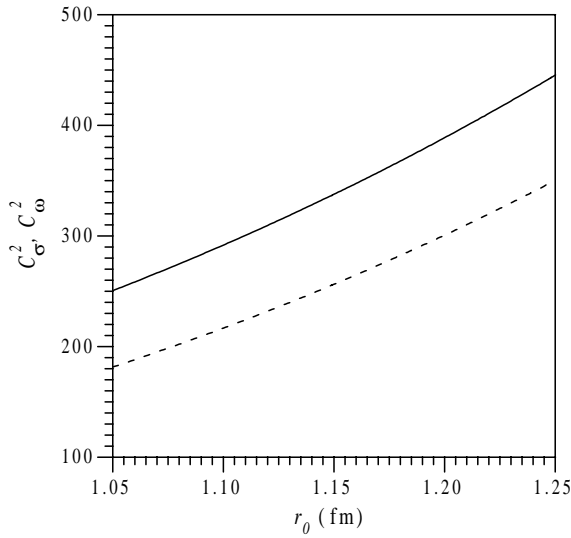


**Fig. 1.** Composite parameters  $C_\sigma^2$  and  $C_\omega^2$  as a function of  $r_0$  for given  $a_1 = 16$  MeV, in the linear  $\sigma$ - $\omega$ - $\rho$  model.

$C_\sigma$  can be solved as a function of  $k_F$  and  $\xi_0$  from eq. (29). Substituting this function of  $C_\sigma$  into the above-mentioned equation, the following equation involving  $e_0$ ,  $k_F$  and  $\xi_0$  can be derived

$$\frac{3}{\xi_0} f_1(k_F/\xi_0 M) + 2f_2(k_F/\xi_0 M) = (e_0 + M) \frac{k_F^3}{\xi_0^4 M^4}. \quad (33)$$

$\xi_0$  can be calculated from this equation, if the location  $(\rho_0, e_0)$  of stable equilibrium point is chosen as input data. Having this  $\xi_0$  together with  $\rho_0$  and  $e_0$ ,  $C_\sigma$  can be calculated from eq. (29), then  $C_\omega$  can be determined from eq. (28) or (30). Finally, the incompressibility  $K_0$  can be obtained from eq. (31). It can be shown easily that eq. (33) is identical to eq. (22) of reference [9] which is originally given in reference [13]. Numerically,  $\rho_0$  and thus  $k_F$  can be expressed in terms of the nuclear radius constant  $r_0$  as eq. (27), while  $e_0$  can be related to the nuclear volume energy coefficient  $a_1$  as  $e_0 = e(\rho_0, 0) = -a_1$ . The experimentally acceptable values are [3]

$$r_0 \approx 1.14 \text{ fm}, \quad a_1 \approx 16 \text{ MeV}. \quad (34)$$

The numerical calculation shows that, in the ranges  $1.05 \text{ fm} \leq r_0 \leq 1.25 \text{ fm}$  and  $15.5 \text{ MeV} \leq a_1 \leq 16.5 \text{ MeV}$ , the effective mass  $\xi \approx 0.54$  does not depend on the choice of  $r_0$  and  $a_1$  sensitively. The composite parameters  $C_\sigma^2$  and  $C_\omega^2$  are sensitive to the choice of  $r_0$  but not of  $a_1$ . Figure 1 shows  $C_\sigma^2$  and  $C_\omega^2$  as a function of  $r_0$  for given  $a_1 = 16$  MeV. Figure 2 gives the nuclear matter incompressibility  $K_0$  calculated by eq. (31) as a function of  $a_1$  for given  $r_0 = 1.14$  fm. It is not sensitive to the choice of  $r_0$ . Furthermore, fig. 2 shows that  $K_0$  is approximately a linear function of  $a_1$ , in agreement with what is obtained in the macroscopic phenomenological approach to the nuclear matter [14].

In case of the Walecka model [15],  $C_\rho = 0$ , other nuclear matter properties  $J$ ,  $L$  and  $K_s$  can be calculated also

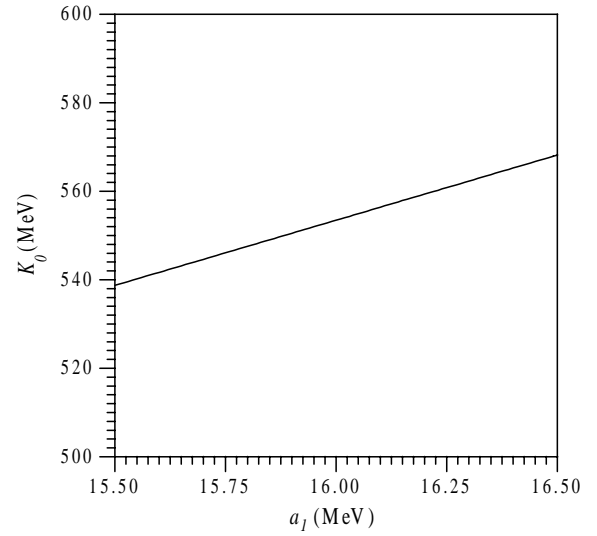


**Fig. 2.** The nuclear matter incompressibility  $K_0$  calculated as a function of  $a_1$  for given  $r_0 = 1.14$  fm, in the linear  $\sigma$ - $\omega$ - $\rho$  model.

from these  $C_\sigma$  and  $C_\omega$  by eqs. (21)–(26). The calculated coefficients  $J$ ,  $L$  and  $K_s$  are almost constant in the range  $15.5 \text{ MeV} \leq a_1 \leq 16.5 \text{ MeV}$  for given  $r_0 = 1.14$  fm,

$$J \approx 20 \text{ MeV}, \quad L \approx 70 \text{ MeV}, \quad K_s \approx 88 \text{ MeV}. \quad (35)$$

On the other hand, these coefficients depend on the choice of  $r_0$  weakly, for given  $a_1$ .

In case  $\rho$ -meson is included also in the model, the composite parameter  $C_\rho$  can be determined by measured symmetry energy  $J$  through eq. (21). The inclusion of  $\rho$ -meson contributes to the symmetry energy with an extra term  $J_\rho$  (eq. (23)) and to the density symmetry  $L$  with an extra term  $3J_\rho$ , while keeping the other coefficients  $a_1$ ,  $K_0$  and  $K_s$  unchanged. For symmetry incompressibility  $K_s$ , it can be seen from eqs. (26) and (14) that the  $\rho$ -meson contributes with a term  $-18J_\rho$  to  $-6L$  and a term  $18J_\rho$  to  $(1/2)\partial^2 K/\partial\delta^2|_0$ , and these extra terms cancel each other.

## 4 Standard state nuclear matter properties

There are many parameter sets for the  $\sigma$ - $\omega$ - $\rho$  model of the relativistic mean-field theory in the literature, some of them are listed in table 1, where L-W is taken from the pioneering Walecka linear  $\sigma$ - $\omega$  model [15], L-HS from the Horowitz-Serot linear  $\sigma$ - $\omega$ - $\rho$  model [16], L1, L2 and L3 from Lee *et al.* [17], L-Z, NL-Z and NL-VT from Rufa *et al.* [18], NL1 from Reinhard *et al.* [19], NL2 from Fink *et al.* [20], NL3 and NL3-II from Lalazissis *et al.* [21], NLB, NLC and NLD from Serot [8], NL-B1 and NL-B2 from Boussy *et al.* [22,23], NL-RA from Rashdan [24], NL-SH from Sharma *et al.* [25], TM1 and TM2 from Sugahara and Toki [26]. Most of them are collected in Reinhard's review [10]. In table 1,  $g_2$  and  $g_3$  are defined, respectively, as

$$g_2 = Mb g_\sigma^3, \quad g_3 = c g_\sigma^4. \quad (36)$$

**Table 1.** Some parameter sets of the  $\sigma$ - $\omega$ - $\rho$  model in the relativistic mean-field theory. See text for details.

Set	$M$	$m_\sigma$	$m_\omega$	$m_\rho$	$g_\sigma$	$g_\omega$	$g_\rho$	$g_2$	$g_3$	$c_3$
L-W	939.0	550.000	783.000	763.	9.57269	11.67114	0.00000	0.00000	0.0000	0.0000
L-HS	939.0	520.000	783.000	770.	10.47026	13.79966	4.03814	0.00000	0.0000	0.0000
L1	938.0	550.000	783.000	763.	10.29990	12.59990	0.00000	0.00000	0.0000	0.0000
L2	938.0	546.940	780.000	763.	11.39720	14.24780	0.00000	0.00000	0.0000	0.0000
L3	938.0	492.260	780.000	763.	10.69200	14.87050	0.00000	0.00000	0.0000	0.0000
L-Z	938.9	551.310	780.000	763.	11.19330	13.82560	5.44415	0.00000	0.0000	0.0000
NL1	938.0	492.250	795.359	763.	10.13770	13.28460	4.97570	12.17240	-36.2646	0.0000
NL2	938.0	504.890	780.000	763.	9.11122	11.49280	5.38660	2.30404	13.7844	0.0000
NL3	939.0	508.194	782.501	763.	10.21700	12.86800	4.47400	10.43086	-28.8849	0.0000
NL3-II	939.0	507.680	781.869	763.	10.20200	12.85400	4.48000	10.39100	-28.9390	0.0000
NLB	939.0	510.000	783.000	770.	9.69588	12.58890	4.27200	2.02714	1.6667	0.0000
NL-B1	938.9	470.000	783.000	770.	8.75834	11.80520	3.75195	7.51446	-16.8112	0.0000
NL-B2	938.9	485.000	783.000	770.	9.72687	12.89370	3.52938	9.47080	-28.1254	0.0000
NLC	939.0	500.800	783.000	770.	9.75244	12.20370	4.32984	12.66960	-33.3333	0.0000
NLD	939.0	476.700	783.000	770.	8.26559	10.86600	4.49305	3.79970	8.3333	0.0000
NL-RA	939.0	515.000	782.600	763.	9.62661	11.90390	4.52418	8.06582	-16.3173	0.0000
NL-SH	939.0	526.059	783.000	763.	10.44400	12.94500	4.38300	6.90990	-15.8337	0.0000
NL-VT	938.9	483.420	780.000	763.	9.79084	12.65660	4.61319	13.16500	-38.1282	0.0000
NL-Z	938.9	488.670	780.000	763.	10.05530	12.90860	4.84944	13.50720	-40.2243	0.0000
TM1	938.0	511.198	783.000	770.	10.02890	12.61390	4.63220	7.23250	0.6183	71.3075
TM2	938.0	526.443	783.000	770.	11.46940	14.63770	4.67830	4.44400	4.6076	84.5318

It should be noted that some of these parameter sets are given originally in values of  $C_i$  instead of  $g_i$ ,  $i = \sigma, \omega, \rho$ . In this case the values of  $g_i$  given here are calculated from  $C_i$ ,  $m_i$  and  $M$  by eq. (9). It should be noted also that our  $g_\rho$  is only one half of that defined in reference [9].

As mainly nuclear matter properties are concerned in the present calculation, the relevant parameters are only  $C_\sigma^2$ ,  $C_\omega^2$ ,  $C_\rho^2$ , while the meson masses  $m_\sigma$ ,  $m_\omega$  and  $m_\rho$  are nonrelevant ones, in case of the linear model. However, in nonlinear model the meson mass is able in some case to influence the nuclear matter property. For example, the  $\omega$ -meson mass  $m_\omega$  appears in eq. (12) and thus has effect on nuclear matter property in the nonlinear model via the term  $(\omega_\mu \omega^\mu)^2$ .

The standard nuclear matter properties related to these parameter sets are shown in table 2, where all quantities are given in MeV, except  $\rho_0$  which is in  $\text{fm}^{-3}$ . In the calculation of  $a_1$ ,  $K_0$ ,  $J$ ,  $L$  and  $K_s$ , using formulas given in section 2 and input parameters listed in table 1, eqs. (11) and (19) should be solved simultaneously at first for  $\xi_0$  and  $k_F$  at the standard point. The calculation of  $\partial^2 K / \partial \delta^2|_0$ , in eq. (26) of  $K_s$ , is made numerically, as its analytical expression is too complicated to be derived. The simple numerical average among the nonlinear model sets is given as the set (NL), and the Myers-Swiatecki's result [4] is shown also as the set MS for comparison.

$\rho_0$  and  $a_1$  give the location of nuclear matter standard state. Most values of  $\rho_0$  given in the  $\sigma$ - $\omega$ - $\rho$  model are lower than that of Myers-Swiatecki's, the later corresponds to  $r_0 = 1.140 \text{ fm}$  and agrees with that obtained from elastic electron scattering and muonic atom spectroscopy measurements [27,28]. Most values of  $a_1$  given in the  $\sigma$ - $\omega$ - $\rho$  model are in the reasonable range around 16 MeV, except those of L1, L2, L3, LZ and NL2 sets, which seem

too large. Since  $a_1$  is the leading term in the approximate equation of state (1), it is the main parameter in any data fit to nuclear masses. However, there is a big fluctuation around 16 MeV, as can be seen from table 2.

$K_0$  and  $J$ , the next terms to the leading  $a_1$  in the approximate equation of state (1), are the fine tune in the data fit to nuclear masses, as shown in the droplet model of nuclei [29]. It can be seen from table 2 that  $K_0$  given in the  $\sigma$ - $\omega$ - $\rho$  model is much larger than that of Myers-Swiatecki's, while  $J$  is only about 2/3 of Myers-Swiatecki's, for the linear  $\sigma$ - $\omega$  model;  $J$  will be increased if the  $\rho$ -meson is added also to the linear  $\sigma$ - $\omega$  model, but  $K_0$  keeps the same value. This is an inherent character of linear  $\sigma$ - $\omega$ - $\rho$  model, as has been shown generally in last section. In this respect, the nonlinear terms are needed in order to reduce the nuclear incompressibility  $K_0$ , as supported by the calculated results listed in table 2. It is worthwhile to note that, even the value of  $K_0$  obtained from different nuclear measurements and astrophysical observations are spread over a large range from 180 to 800 MeV [30], most expectations based on the non-relativistic model are around 220 MeV [11].

Being terms of order higher than  $K_0$  and  $J$  in the approximate equation of state (1),  $L$  and  $K_s$  belong to the superfine tune in the data fit to nuclear masses. Even if most values of  $L$  given in the  $\sigma$ - $\omega$ - $\rho$  model seem to be larger than the acceptable one, they are still in the reasonable range around 100 MeV. On the other hand, the values of  $K_s$  are all positive whose sign is opposite to most expectations based on the nonrelativistic model [1]. Experimentally,  $K_s$  obtained from the isoscalar giant-monopole resonance energy is between  $-566 \pm 1350$  to  $34 \pm 159 \text{ MeV}$  [31].

**Table 2.** Standard nuclear matter properties given by the  $\sigma$ - $\omega$ - $\rho$  model parameter sets listed in table 1.  $a_1$ ,  $K_0$ ,  $J$ ,  $L$  and  $K_s$  are in MeV,  $\rho_0$  in  $\text{fm}^{-3}$ . See text for details.

Set	$\rho_0$	$a_1$	$K_0$	$J$	$L$	$K_s$
L-W	0.1937	15.75	545.6	22.11	74.5	74.8
L-HS	0.1485	15.75	546.8	34.98	115.5	93.4
L1	0.1766	18.52	625.6	21.68	75.6	81.8
L2	0.1417	16.78	578.5	19.07	68.8	97.4
L3	0.1344	18.24	624.5	18.86	69.5	102.1
L-Z	0.1494	17.07	586.3	48.84	157.9	94.2
NL1	0.1518	16.42	211.1	43.46	140.1	142.6
NL2	0.1456	17.03	399.4	43.86	129.7	20.1
NL3	0.1482	16.24	271.6	37.40	118.5	100.8
NL3-II	0.1491	16.26	271.7	37.70	119.7	103.3
NLB	0.1485	15.77	421.0	35.01	108.3	54.8
NL-B1	0.1625	15.79	280.4	33.04	102.5	76.1
NL-B2	0.1627	15.79	245.6	33.10	111.3	158.8
NLC	0.1485	15.77	224.4	35.02	108.0	76.8
NLD	0.1485	15.77	343.2	35.01	101.5	13.5
NL-RA	0.1570	16.25	320.5	38.90	119.1	62.0
NL-SH	0.1460	16.35	355.3	36.12	113.6	79.7
NL-VT	0.1530	16.09	172.8	39.73	126.9	130.0
NL-Z	0.1508	16.19	172.8	41.72	133.9	140.0
TM1	0.1452	16.26	281.2	36.89	110.8	33.5
TM2	0.1323	16.16	343.8	35.98	113.0	56.0
(NL)	0.1500	16.14	287.7	37.53	117.1	83.2
MS	0.1611	16.24	234.4	32.65	49.9	-147.1

## 5 Prediction for cold nuclear matter under extreme conditions

The stability condition for the state at minimum of equation of state for given asymmetry  $\delta$  is

$$p(\rho_m, \delta) = 0. \quad (37)$$

The solution of this equation for given  $\delta$  gives the location of the minimum  $\rho_m = \rho_m(\delta)$ . Knowing this location  $\rho_m(\delta)$ , the minimum  $e_m = e(\rho_m, \delta)$  and the generalized incompressibility at this minimum  $K_m(\delta) = K(\rho_m, \delta)$  can be calculated. Furthermore, the critical point of the equation of state  $(\rho_c, \delta_c)$  can be defined as the point where the maximum and the minimum are coincident and thus the curvature of  $e(\rho, \delta_c)$  versus  $\rho$  equals zero. As the generalized incompressibility  $K(\rho, \delta)$  is proportional to this curvature, we have at the critical point

$$K_m(\delta_c) = K(\rho_c, \delta_c) = 0. \quad (38)$$

This equation together with (37) can be used to obtain the critical point  $(\rho_c, \delta_c)$ .

Table 3 lists the calculated critical point  $(\rho_c, \delta_c)$ , the corresponding effective nucleon mass  $M^*/M$ , the energy per nucleon  $e_m$  as well as the generalized incompressibility  $K_m$  at the critical point. In case there is no critical point, the corresponding quantities at the minimum point of the pure neutron matter equation of state with  $\delta = 1$  are listed.  $\rho_c$  is in  $\text{fm}^{-3}$  units, while  $e_m$  and  $K_m$  are in MeV units. The values given by the Myers-Swiatecki equation of state [11] are also listed in the last row for comparison.

It can be seen that there is no critical point for parameter sets LW, L1, L2, L3 and NL-B2. In these cases, there is a minimum for the pure neutron matter equation of state and the bound neutron matter is predicted. For other parameter sets, the neutron matter is an unbound gas system. The predicted critical point  $(\rho_c, \delta_c)$  is in the ranges  $0.014 \text{ fm}^{-3} < \rho_c \leq 0.039 \text{ fm}^{-3}$  and  $0.74 < \delta_c \leq 0.95$ , with the corresponding effective nucleon mass in the range  $0.87 \leq M^*/M \leq 0.95$ .

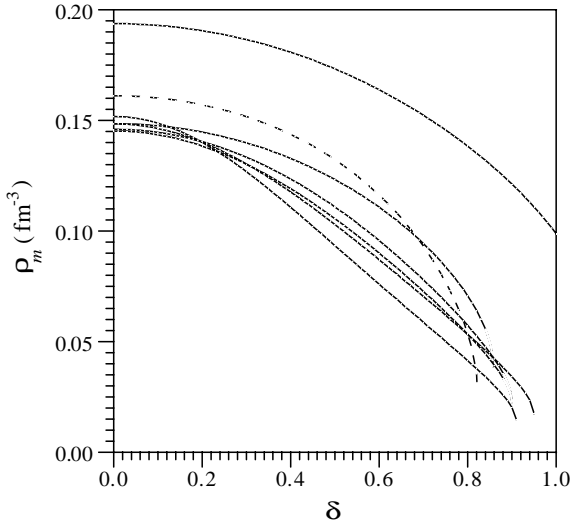
In addition, the predicted maximum mass  $M_{\text{NS}}$  and the corresponding radius  $R_{\text{NS}}$  of neutron stars, calculated by the Oppenheimer-Volkoff equation, using the  $\sigma$ - $\omega$ - $\rho$  model equation of state of the relativistic mean-field theory with the above-mentioned parameter sets and  $\delta = 1$ , are also shown in table 3. The range of the maximum mass is  $2.45M_\odot \leq M_{\text{NS}} \leq 3.26M_\odot$ , and the range of corresponding star radius is  $12.2 \text{ km} \leq R_{\text{NS}} \leq 15.1 \text{ km}$ .

Figure 3 gives some examples of  $\rho_m(\delta)$ , where the solid curve from top to bottom in the middle range of  $\delta$  corresponds to L-W, L-HS, NL-SH, TM1, NLC, and NL1; the dashed curve corresponds to Myers-Swiatecki's result. One source of deviation among these curves comes from the difference in the origin of the curves:  $\rho_0 = \rho_m(0)$ . In cases of L-W and L1  $\rho_0$  is much higher but others are close or lower than that of Myers-Swiatecki's. However, even if all the curves are rescaled to the same  $\rho_0$ , there still exists large deviation among these curves in the middle range of  $\delta$ .

Figure 4 plots some examples of  $e_m$  versus  $\delta$ , where the solid curve from left to right on the end of the curve corresponds to L-HS, NL-SH, TM1, NL1, NLC, and L-W; the

**Table 3.** Nuclear matter properties at the critical point  $(\rho_c, \delta_c)$  or  $(\rho_m, 1)$ , the maximum neutron star mass  $M_{\text{NS}}$  and the corresponding star radius  $R_{\text{NS}}$ , calculated by the  $\sigma$ - $\omega$ - $\rho$  model parameter sets listed in table 1.  $\rho_c$  is in  $\text{fm}^{-3}$ ,  $e_c$  and  $K_c$  in MeV,  $M_{\text{NS}}$  in solar mass  $M_{\odot}$  and  $R_{\text{NS}}$  in km. Myers-Swiatecki's values are listed in the last row for comparison. See text for details.

Set	$\delta_c$	$\rho_c$	$M^*/M$	$e_c$	$K_c$	$M_{\text{NS}}$	$R_{\text{NS}}$
L-W	1.00	0.0987	0.766	1.93	77.8	2.60	12.2
L-HS	0.86	0.0392	0.872	2.75	0.0	3.08	14.6
L1	1.00	0.1034	0.718	-0.63	142.3	2.80	13.0
L2	1.00	0.0849	0.712	-1.04	138.4	3.13	14.4
L3	1.00	0.0847	0.688	-2.46	174.5	3.26	15.0
L-Z	0.75	0.0388	0.871	2.51	0.0	3.16	15.1
NL1	0.91	0.0150	0.951	1.43	0.0	2.96	14.2
NL2	0.81	0.0288	0.925	2.41	0.0	2.78	13.9
NL3	0.92	0.0182	0.943	1.62	0.0	2.91	13.9
NL3-II	0.92	0.0178	0.944	1.62	0.0	2.91	13.9
NLB	0.87	0.0327	0.906	2.43	0.0	2.87	13.8
NL-B1	0.95	0.0236	0.936	1.94	0.0	2.68	12.9
NL-B2	1.00	0.0212	0.934	1.75	1.8	2.87	13.5
NLC	0.95	0.0175	0.949	1.63	0.0	2.77	13.2
NLD	0.87	0.0302	0.929	2.29	0.0	2.60	13.0
NL-RA	0.87	0.0243	0.934	1.89	0.0	2.75	13.4
NL-SH	0.90	0.0235	0.927	1.90	0.0	2.93	14.1
NL-VT	0.95	0.0151	0.952	1.44	0.0	2.87	13.7
NL-Z	0.94	0.0144	0.953	1.39	0.0	2.92	13.9
TM1	0.90	0.0217	0.935	1.82	0.0	2.45	13.3
TM2	0.90	0.0217	0.918	1.83	0.0	2.73	14.4
MS	0.82	0.0304		1.10	0.0		



**Fig. 3.** Some examples of the location  $\rho_m(\delta)$  of the  $\sigma$ - $\omega$ - $\rho$  model equation of state. The solid curves from top to bottom in the middle range of  $\delta$  correspond to L-W, L-HS, NL-SH, TM1, NLC, and NL1, respectively. The dashed curve corresponds to Myers-Swiatecki's result.

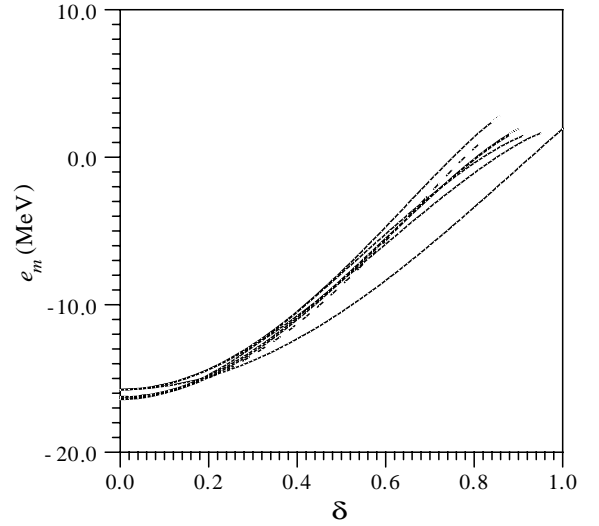


**Fig. 4.** Some examples of the deep  $e_m \times \delta$  of the  $\sigma$ - $\omega$ - $\rho$  model equation of state. The solid curves from left to right on the high  $\delta$  range correspond to L-HS, NL-SH, TM1, NL1, NLC, and L-W, respectively. The dashed curve corresponds to Myers-Swiatecki's result.

dashed curve corresponds to Myers-Swiatecki's result. All curves are close each other in the low asymmetry region, but L-W's is significantly lower than others for  $\delta > 0.2$ .

Figure 5 is the curve  $K_m$  versus  $\delta$  calculated by same parameter sets as that of figs. 3 and 4. The solid curve

from top to bottom in the middle range of  $\delta$  is by L-W, L-HS, NL-SH, TM1, NLC, and NL1, and the dashed curve is by Myers-Swiatecki. The difference between these curves is obvious, even if NLC and NL1's are close to each other as well as close to Myers-Swiatecki's.

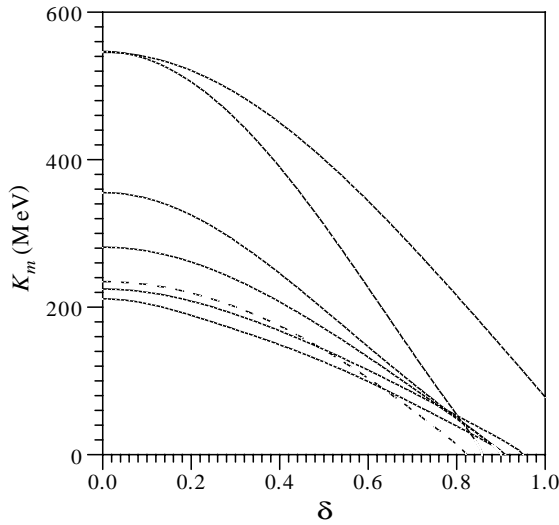


**Fig. 5.** The curve  $K_m \times \delta$  calculated by the same  $\sigma$ - $\omega$ - $\rho$  model parameter sets as shown in figs. 4 and 5. The solid curves from top to bottom in the middle range of  $\delta$  correspond to L-W, L-HS, NL-SH, TM1, NLC, and NL1, respectively, and the dashed curve corresponds to Myers-Swiatecki's result.

## 6 Summary

In summary, the properties of nuclear matter at standard density  $\rho_0$  with equal neutron and proton densities,  $\rho_n = \rho_p$ , are calculated at first in the relativistic mean-field theory with a variety of parameter sets. The result shows that the volume energy  $a_1$  and symmetry energy  $J$  are around the acceptable value 16 MeV and 30 MeV respectively, the incompressibility  $K_0$  is reasonable only for nonlinear model while is unacceptably high for linear model, the density symmetry  $L$  is around 100 MeV for most parameter sets, and the symmetry incompressibility  $K_s$  has positive value whose sign is opposite to most expectations based on the nonrelativistic model.

Secondly, the calculation shows that for most parameter sets there exists a critical point  $(\rho_c, \delta_c)$ , where the minimum and the maximum of the equation of state are coincident and the incompressibility equals zero, and it falls into ranges  $0.014 \text{ fm}^{-3} < \rho_c < 0.039 \text{ fm}^{-3}$  and  $0.74 < \delta_c \leq 0.95$ ; while for some parameter sets there is no critical point and the pure neutron matter is bound. The deviation among results calculated by different parameter sets is discussed. The maximum mass of neutron stars is also calculated with results in the range  $2.45 M_\odot \leq M_{\text{NS}} \leq 3.26 M_\odot$ . It is worthwhile to note that a more realistic calculation, by using a nuclear Thomas-Fermi equation of state, gives a maximum mass of neutron stars equal to  $3.26 M_\odot$  [32]. The most of observational neutron star masses are between  $1.2$ – $1.8 M_\odot$ .

As different parameter sets give results which deviate significantly from one another, in order to extract from them more reliable predictions for nuclear matter properties, more sophisticated data fit, especially the data fit to larger number of nuclear masses and other measured

nuclear data is expected for the nonlinear  $\sigma$ - $\omega$ - $\rho$  model of relativistic mean-field theory.

## Appendix A.

Functions  $F_m(x)$  and  $f_m(x)$  defined below are useful in the analytical expressions and numerical calculations of the relativistic mean-field theory:

$$F_m(x) \equiv \int_0^x dx \cdot x^{2m} \sqrt{1+x^2}, \quad m \geq 1, \quad (\text{A.1})$$

$$f_m(x) \equiv \int_0^x dx \frac{x^{2m}}{\sqrt{1+x^2}}, \quad m \geq 1. \quad (\text{A.2})$$

The following formulas can be obtained:

$$F_m(x) = f_m(x) + f_{m+1}(x), \quad (\text{A.3})$$

$$f'_{m+1}(x) = x^2 f'_m(x), \quad (\text{A.4})$$

$$F'_{m+1}(x) = x^2 F'_m(x), \quad (\text{A.5})$$

$$F'_m(x) = (1+x^2) f'_m(x), \quad (\text{A.6})$$

$$f_m(x) = x F'_{m-1}(x) - (2m-1) F_{m-1}(x), \quad (\text{A.7})$$

$$f_m(x) = -x F'_m(x) + 2(m+1) F_m(x). \quad (\text{A.8})$$

Some examples of  $F_m(x)$  and  $f_m(x)$  are

$$F_1(x) = \frac{1}{8} \left[ (1+2x^2)x\sqrt{1+x^2} + \ln(\sqrt{1+x^2}-x) \right], \quad (\text{A.9})$$

$$f_1(x) = \frac{1}{2} \left[ x\sqrt{1+x^2} + \ln(\sqrt{1+x^2}-x) \right], \quad (\text{A.10})$$

$$f_2(x) = -\frac{3}{8} \left[ \left(1 - \frac{2}{3}x^2\right)x\sqrt{1+x^2} + \ln(\sqrt{1+x^2}-x) \right]. \quad (\text{A.11})$$

For  $x \ll 1$ , we have

$$F_m(x) = \frac{x^{2m+1}}{2m+1} + \frac{x^{2m+3}}{2(2m+3)} - \frac{x^{2m+5}}{8(2m+5)} + \dots, \quad (\text{A.12})$$

$$f_m(x) = \frac{x^{2m+1}}{2m+1} - \frac{x^{2m+3}}{2(2m+3)} + \frac{3x^{2m+5}}{8(2m+5)} + \dots. \quad (\text{A.13})$$

## References

1. B.A. Li, C.M. Ko, W. Bauer, Int. J. Mod. Phys. E **7**, 147 (1998).
2. W.D. Myers, W.J. Swiatecki, Ann. Phys. (N.Y.) **55**, 395 (1969).
3. K.C. Chung, C.S. Wang, A.J. Santiago, J.W. Zhang, Phys. Rev. C **61**, 047303 (2000).



4. W.D. Myers, W.J. Swiatecki, Nucl. Phys. A **601**, 141 (1996).
5. K.C. Chung, C.S. Wang, A.J. Santiago, Europhys. Lett. **47**, 663 (1999).
6. C.S. Wang, K.C. Chung, A.J. Santiago, Phys. Rev. C **60**, 034310 (1999).
7. B.D. Serot, J.D. Walecka, Adv. Nucl. Phys. **16**, 1 (1986).
8. B.D. Serot, Rep. Prog. Phys. **55**, 1855 (1992).
9. B.D. Serot, J.D. Walecka, Int. J. Mod. Phys. E **6**, 515 (1997).
10. P.G. Reinhard, Rep. Prog. Phys. **52**, 439 (1989).
11. W.D. Myers, W.J. Swiatecki, Phys. Rev. C **57**, 3020 (1998).
12. J.D. Bjorken, S.D. Drell, *Relativistic Quantum Fields*, (McGraw-Hill, New York, 1965).
13. R.J. Furnstahl, B.D. Serot, H.-B. Tang, Nucl. Phys. A **598**, 539 (1996).
14. K.C. Chung, C.S. Wang, A.J. Santiago, J.W. Zhang, *Effective nucleon-nucleon interactions and nuclear matter equation of state*, to be published in Eur. J. Phys. A.
15. J.D. Walecka, Ann. Phys. (N.Y.) **83**, 491 (1974).
16. C.J. Horowitz, B.D. Serot, Nucl. Phys. A **368**, 503 (1981).
17. S.-J. Lee, J. Fink, A.B. Balantekin, M.R. Strayer, A.S. Umar, P.-G. Reinhard, J.A. Maruhn, W. Greiner, Phys. Rev. Lett. **57**, 2916 (1986); **59**, 1171 (1986).
18. M. Rufa, P.-G. Reinhard, J. Maruhn, W. Greiner, M.R. Strayer, Phys. Rev. C **35**, 390 (1988).
19. P.-G. Reinhard, M. Rufa, J. Maruhn, W. Greiner, J. Friedrich, Z. Phys. A **323**, 13 (1986).
20. J. Fink, S.-J. Lee, A.S. Umar, M.R. Strayer, J.A. Maruhn, W. Greiner, P.-G. Reinhard, ORNL Preprint, 1988.
21. G.A. Lalazissis, J. König, P. Ring, Phys. Rev. C **55**, 540 (1997).
22. A. Boussy, S. Marcos, J.F. Mathiot, Nucl. Phys. A **415**, 497 (1984).
23. A. Boussy, S. Marcos, Pham van Thieu, Nucl. Phys. A **422**, 541 (1984).
24. M. Rashdan, Phys. Lett. B **395**, 141 (1997).
25. M.M. Sharma, M.A. Nagarajan, P. Ring, Phys. Lett. B **312**, 377 (1993).
26. Y. Sugahara, H. Toki, Nucl. Phys. A **579**, 557 (1994).
27. H. de Vries, C.W. de Jager, C. de Vries, At. Data Nucl. Data Tables **36**, 495 (1987).
28. G. Fricke, C. Bernhardt, K. Heilig, L.A. Schaller, L. Schellenberg, E.B. Shera, C.W. de Jager, At. Data Nucl. Data Tables **60**, 177 (1995).
29. W.D. Myers, *Droplet Model of Atomic Nuclei* (IFI/Plenum, New York, 1977).
30. N.K. Glendenning, Phys. Rev. C **37**, 2733 (1988).
31. S. Shlomo, D.H. Youngblood, Phys. Rev. C **47**, 529 (1993).
32. K.C. Chung, T. Kodama, Braz. J. Phys. **8**, 404 (1978).